optica

Quantum-enhanced tomography of unitary processes: supplementary material

Xiao-Qi Zhou*, Hugo Cable*, Rebecca Whittaker*, Peter Shadbolt, Jeremy L. O'Brien, and Jonathan C. F. Matthews

Centre for Quantum Photonics, H. H. Wills Physics Laboratory and Department of Electrical and Electronic Engineering, University of Bristol, Merchant Venturers Building, Woodland Road, Bristol BS8 1UB, UK

* *These authors contributed equally*

Published 25 May 2015

This document provides supplementary material for "Quantum-enhanced tomography of unitary pro-cesses," http://dx.doi.org/10.1364/optica.2.000510.

http://dx.doi.org/10.1364/optica.2.000510

1. PARAMETER DEPENDENCE OF THE PROBABILITY DISTRIBUTIONS FOR MEASUREMENTS IN A FIXED BASIS

Here we identify what information is obtainable from each measurement in our protocol, for an arbitrary (unitary) linear-optical process $\mathcal{U}$ on two modes. The action of $\mathcal{U}$ on the mode operators is given by,

$$\begin{pmatrix} a_H'^\dagger \\ a_V'^\dagger \end{pmatrix} = \begin{pmatrix} \mathcal{U} a_H^\dagger \mathcal{U}^\dagger \\ \mathcal{U} a_V^\dagger \mathcal{U}^\dagger \end{pmatrix} = U^t \begin{pmatrix} a_H^\dagger \\ a_V^\dagger \end{pmatrix} \tag{S1}$$

where U is a unitary two-by-two matrix. The global phase of $\mathcal{U}$ is unmeasurable in our setup and hence we assume $U \in SU(2)$.

U also corresponds to the linear transformation by $\mathcal{U}$ of an arbitrary single-photon superposition state in the Fock basis, $|\psi_1\rangle = c_H|1,0\rangle_{HV} + c_V|0,1\rangle_{HV}$, so that $|\psi_1\rangle \mapsto \mathcal{U}|\psi_1\rangle$ is given by $\left(\begin{smallmatrix} c_H \\ c_V \end{smallmatrix}\right) \mapsto U \left(\begin{smallmatrix} c_H \\ c_V \end{smallmatrix}\right)$. We can represent $|\psi_1\rangle$ geometrically on the Bloch sphere with $|0\rangle \equiv |H\rangle$ and $|1\rangle \equiv |V\rangle$ in the usual qubit notation. $\mathcal{U}$ then acts by rotating the Bloch vector of $|\psi_1\rangle$ by an angle ϕ around the rotation axis with unit vector $\boldsymbol{n}$, where $U = \exp\left[-i(\phi/2)\mathbf{n}\cdot\boldsymbol{\sigma}\right]$ ($\boldsymbol{\sigma} = (\sigma_x, \sigma_y, \sigma_z)$ denotes the Pauli matrices). For an arbitrary N-photon state, $|\psi_N\rangle = \sum_{M=0}^{N} c_M a_H^{\dagger M} a_V^{\dagger N-M} |\text{vac}\rangle$, $\mathcal{U}|\psi_N\rangle = \sum_{M=0}^{N} c_M \left(a_H'^\dagger\right)^M \left(a_V'^\dagger\right)^{N-M} |\text{vac}\rangle$, and again the transformation is determined entirely by the coefficients of U.

Next we look at the general form of the probability distributions for measuring $n_{H(V)}$ horizontally (vertically)-polarized photons at the output, given state $|M, N-M\rangle_{HV}$ at the input, with notation $\mathcal{P}_{HV}(n_H, n_V) = |\langle n_H, n_V|_{HV}\mathcal{U}|M, N-M\rangle_{HV}|^2$. ($M = N/2$ in the main text.) We can use an Euler-angle decomposition to write U as a sequence of rotations on the Bloch sphere about the y and z axes: $U = \left[-i(\psi/2)\sigma_z\right] \exp\left[-i(\theta/2)\sigma_y\right] \exp\left[-i(\zeta/2)\sigma_z\right]$. The z-axis rotations generate phases which do not affect the value of $\mathcal{P}_{HV}(n_H, n_V)$, which therefore depends only on the y-axis rotation with angle θ. As in the main text, we can use p_{HV} to parameterize $\mathcal{P}_{HV}(n_H, n_V)$, and $p_{HV} = \cos^2(\theta/2)$. The probability distributions are given explicitly by rotational Wigner d-matrices as follows,

$$\mathcal{P}_{HV}(n_H, n_V, p_{HV}) = \left[d^{\frac{N}{2}}_{\frac{n_H}{2} - \frac{n_V}{2}, M - \frac{N}{2}} \left(2 \arccos \sqrt{p_{HV}}\right) \right]^2. \tag{S2}$$

(see Ref. [1] for a derivation of the d-matrices). For the case $M = N/2$, $\mathcal{P}_{HV}(n_H, n_V, p_{HV})$ can be reexpressed using the associated Legendre polynomials as given explicitly in Eq. 3 in the main text.

We note that even the full set of unitaries which are implementable using linear-optical circuits on arbitrary numbers of modes does not exhaust all unitary operations of interest for quantum information protocols. In particular, a full set of circuits suitable for universal quantum computing cannot be achieved using only linear optics. However, when linear-optical components are combined with feed-forward techniques, photon-counting measurements and single-photon sources, universal quantum computation is achievable [2], and the techniques developed in this paper could be used to characterize the linear-optical components in architectures which exploit measurement-induced nonlinearity. For example, a Controlled-NOT gate can be realised by a linear-optical circuit on six modes with photon detectors at the outputs of two modes [3, 4].

2. PERFORMANCE OF OUR PROTOCOL WITH INCREASING NUMBER OF PROBE PHOTONS

Here we present the performance of our protocol for a variety of unknown $\mathcal{U}$ and varying numbers of probe photons. To quantify the closeness of an estimate of $\tilde{U}$ to U itself we use the process infidelity $1 - F$, defined as in the main text as $\left(1 - \min|\langle\psi|\tilde{U}^\dagger U|\psi\rangle|^2\right)$, where the minimization is over single-photon states. A closed formula can be found for this minimization which is $1 - F = 1 - \left(a\tilde{a} + b\tilde{b} + c\tilde{c} + d\tilde{d}\right)^2$,

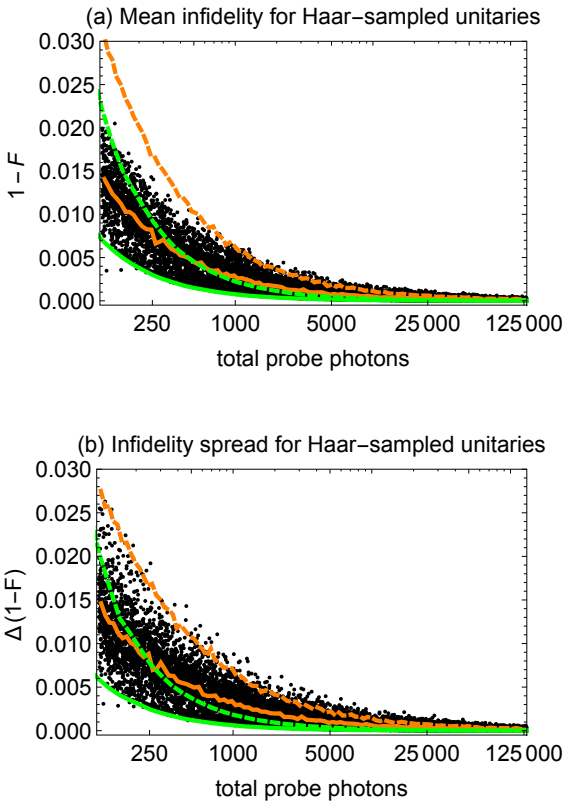

Fig. S1. These plots display the results of a simulation of our protocol for 10,000 randomly-chosen unitary operations (using the Haar-measure distribution). Each black point corresponds to one unitary, and a randomly-chosen number of total probe photons, with four-photon input states $|2,2\rangle_{HV(DA,RL)}$ as the probe. The solid green line shows the performance for unitaries at the centre of the physical region, for which $|a| = |b| = |c| = |d| = 1/2$, while the solid orange line shows the average performance for all the unitaries that were sampled. The dashed green and orange lines show the corresponding performance when single-photon input states are used in place of the four-photon inputs.

where $a + ib$ and $c + id$ are the transmission and reflection amplitudes for U, and $\tilde{a} + i\tilde{b}$ and $\tilde{c} + i\tilde{d}$ are the corresponding estimated values.

Fig. S1 shows the performance of our protocol for randomly-chosen U using four-photon input states. The choice of U affects both the sensitivity of each of the measurements used in the protocol, as well as the proportion of estimates (by linear inversion) that lie in the physical region; both of these factors affect the mean and spread of the infidelity (for a fixed total number of probe photons). Here we note that, because the most sensitive unitary is known (see the caption of Fig. S1), we can always achieve near-optimal performance (green, solid line shown in Fig. S1) by combining our protocol with an adaptive method. Fig. S2 compares the results of a simulation of the performance of our protocol with unitaries U_A and U_B for single and four-photon inputs states, showing how the mean and spread of the infidelity converge to 0 as the number of probe photons increases. We can observe that the errors for estimating each unitary are always less using the four-photon input states in our protocol than when single-photon input states are used (for the same number of probe photons).

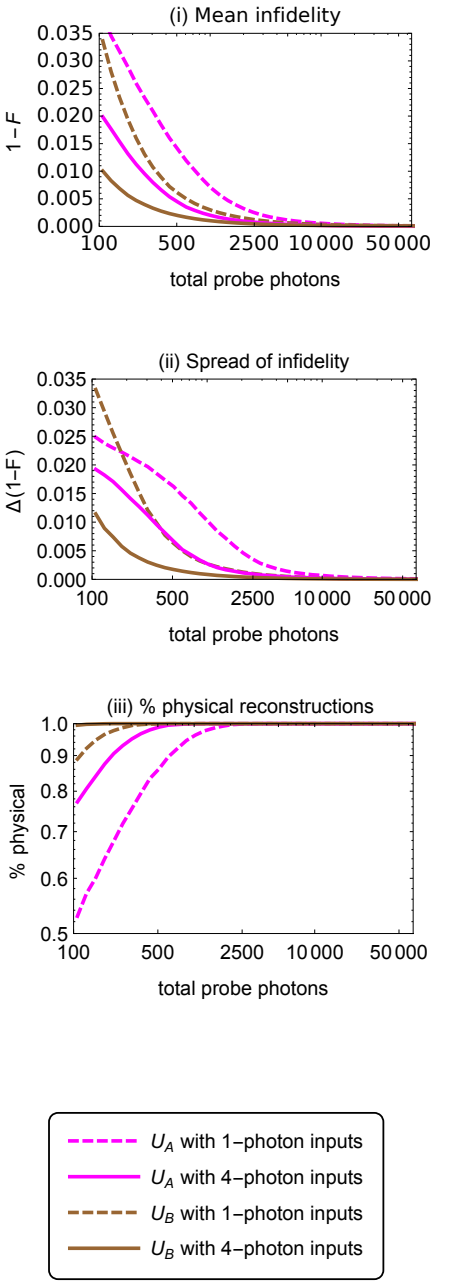

Fig. S2. The plots show the results of a simulation of the performance of our protocol for unitaries U_A and U_B, defined by comparing the cases of single-photon inputs states $|1,0\rangle_{HV(DA,RL)}$ and four-photon input states, $|2,2\rangle_{HV(DA,RL)}$.

REFERENCES

1. J. J. Sakurai, *Modern Quantum Mechanics* (Addison Wesley, 1994), vol. 1, chap. 3.8.
2. E. Knill, R. Laflamme, and G. J. Milburn, "A scheme for efficient quantum computation with linear optics," Nature **409**, 46–52 (2001).
3. T. C. Ralph, N. K. Langford, T. B. Bell, and A. G. White, "Linear optical controlled-NOT gate in the coincidence basis," Phys. Rev. A **65**, 062324 (2001).
4. A. Politi, *et al.*, "Silica-on-silicon waveguide quantum circuits," Science **320**, 646–649 (2008).